

# Correlated Roughness in Polymer Films Containing Magnetic Nanoparticles

M.M. Abul Kashem, J. Perlich, L. Schulz, S.V. Roth\* and P. Müller-Buschbaum

TU München, Physik Department LS E13, James-Franck-Str.1, 85747 Garching, Germany  
\*HASYLAB at DESY, Notke Str. 85, 22603 Hamburg, Germany

## ABSTRACT

Long-range interface correlations in nanocomposite films of a diblock copolymer matrix with embedded magnetic nanoparticles are investigated. A film thickness gradient representing a combinatorial approach to probe samples with different thicknesses prepared under identical conditions is addressed. Maghemite ( $F_2O_3$ ) nanoparticles covered with polystyrene chains are incorporated in a thin film gradient of polystyrene-block-polyisoprene. The gradient is investigated with scanning micro-focus grazing incident small angle X-ray scattering ( $\mu$ GISAXS). The substrate surface roughness is imposed to the composite film surface resulting in roughness correlation. With decreasing film thickness this long-range interface correlation decays.

**Keywords:** correlated roughness, GISAXS, nanocomposite

## 1 INTRODUCTION

Nanocomposite materials based on a polymeric matrix and inorganic fillers is a topic of research in several different areas including standard fillers such as carbon black, clay and silica. The advantages of nanocomposite materials such as achieving desired mechanical, electrical and thermal properties have been reported since long [1, 2]. Rendering magnetic properties to the polymer by using magnetic nanoparticles in the diblock copolymer films is a rather new idea [3]. In addition, the surface topography of thin films influences typical characteristics of nanocomposites [4]. Constant film thickness is of very high importance in technical applications such as protective coatings in microelectronics and optics. Polymer films of uniform thickness on top of solid support can be produced by the widely used spin-coating technique. A broad range of film thicknesses (from the sub-monolayer regime up to several micrometers) are accessible by varying the preparation parameters such as the concentration of the polymer solution, the molecular weight of the polymer and the rotation speed. However, the uniformity of the film thickness, which is produced by spin-coating, is thought in a statistical meaning in terms of an average value. Local deviations from this mean value are given by the roughness. In case of thin films, both roughnesses the substrate and the surface roughness of the film have to be considered. As a consequence, on a local position deviations from the mean film thickness are present. In particular, at some positions the local thickness is smaller than the mean thickness and

thus the protective effect might be not sufficient at these spots. With respect to application these deviations force the necessity to account for this and e.g. produce thicker films which requires more material. The installation of long-range interface correlations offers an approach to overcome this problem.

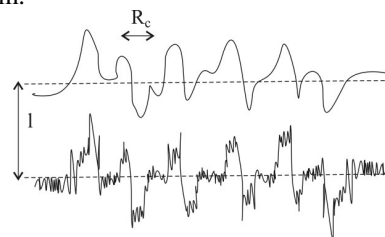


**Figure 1.** Schematic drawing (side view) of roughness replication from a substrate to the top of a film coated on it. The mean film thickness  $l$  is determined by standard X-ray reflectivity measurements. The in-plane cut-off length  $R_c$  determines the part of the roughness spectrum replicated by the film, i.e. only in-plane length scales larger than  $R_c$  are transferred to the film interface. The amplitude of the roughness spectrum is highly exaggerated for clarity.

Because the solid substrate has a given topography the film should exhibit the similar topography to have a locally well defined film thickness. This replication of topography is identical with a replication of the roughness spectrum from the solid substrate through a thin film surface. It results in a correlation among both [4-10]. Perfect correlation between a substrate and the film upon it is called 'conformal' roughness. Figure 1 shows schematically this roughness correlation between the thin film and the substrate underneath. In literature, interface correlation was observed in different thin polymer films, such as single films or multilayers [4-6], thin solid films [7-8], Langmuir-Blodgett films [9-10] and smectic films [11-12]. It was observed, that roughness correlation in thin polymer films decays with a long annealing time [5]. Below the entanglement molecular weight not long-ranged interface correlation was observed [5]. However, at high molecular weights the chain structure tends to weaken roughness correlation as well. Thus to obtain roughness correlation and thus a locally well defined film thickness an intermediate regime of molecular weights seems optimal.

Within the present investigation we focus on roughness correlation between a Si substrate and nanocomposite films with a diblock copolymer matrix and embedded magnetic nanoparticles. We address the effect of film thickness. Instead of the preparation and investigation of several individual nanocomposite films which differ in film

thickness, we adapt a combinatorial approach which is based on a film thickness gradient. To the best of our knowledge, so far there is no report on roughness correlation in polymer composite films containing magnetic nanoparticles. Moreover, due to the gradient approach all different film thicknesses are prepared under exactly identical conditions, which is especially in case of composite films very important. To be able to access the gradient, the investigation was carried out by scanning micro-focus grazing incident small angle X-ray scattering ( $\mu$ GISAXS). The grazing incidence geometry enhances the surface sensitivity and overcomes the limitations of conventional small angle x-ray scattering studies regarding extremely small sample volumes in the thin film geometry [13].

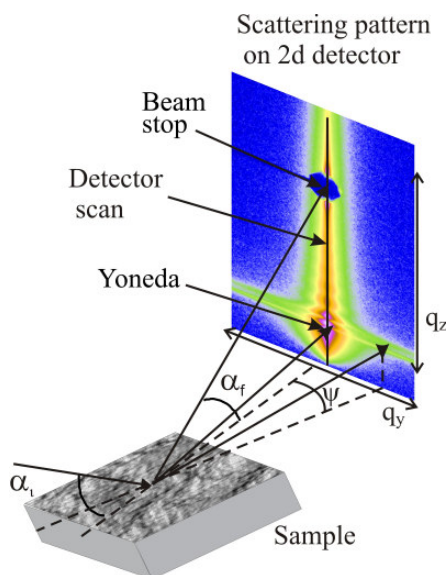


**Figure 2.** Schematic picture of the experimental set-up in GISAXS geometry: The sample surface is placed horizontally. The incident angle is denoted  $\alpha_i$ , the exit angle  $\alpha_f$ , and the out-of-plane angle  $\psi$ . The two-dimensional detector resembles along the horizontal axis the  $q_y$  dependence and along the vertical axis the  $q_z$  dependence (neglecting a small  $q_x$  dependence). The scattering intensity distribution on the detector (low intensity as dark and high intensity as bright) is presented in a logarithmic scale. The detected scattering pattern shows the diffuse scattering with modulations of the intensity between Yoneda peak and specular peak (shielded by a beam-stop that protects the detector from a very high intensity of the reflected beam).

## 2 EXPERIMENTAL SECTION

### 2.1 Sample preparation

We have used the symmetric diblock copolymer polystyrene-block-polyisoprene, denoted P(S-b-I), with a molecular weight  $M_w=24.500$  g/mol having a volume fraction of PS  $f_{PS}=N_{PS}/N=0.56$ . In the bulk this polymer has a lamellar morphology. Maghemite nanoparticles ( $Fe_2O_3$ )

with a mean diameter of 11 nm (20% size distribution), covered with polystyrene chains were used as filler in the polymer matrix. A polymer solution (polymer concentration 10 mg/ml toluene) containing 25 % (wt) nanoparticles as a dispersion was used for the film preparation. The thickness gradient was produced by spin coating the mixture on pre-cleaned silicon (100) substrates covered by a native oxide layer. The cleaning of the substrates used an acidic bath (160 ml of 96% sulfuric acid, 70 ml of 30% hydrogen peroxide and 110 ml of deionized water) at 80°C followed by strong rinsing with deionized water immediately before coating. A gradient in thickness ranging from 10 nm to 700 nm was achieved as measured by atomic force microscopy (AFM). No further processing was applied. The surface topography was imaged by optical microscopy and AFM.

### 2.2 $\mu$ GISAXS

To probe the roughness correlation together with structures present on top and inside the nanocomposite gradient the surface sensitive X-ray scattering technique grazing incident small angle X-ray scattering (GISAXS) was used. The basic set-up of the GISAXS scattering geometry is shown schematically in figure 2. To access the gradient scanning micro-focus GISAXS ( $\mu$ GISAXS) measurements were carried out at the beamline BW4 of the DORIS III storage ring at HASYLAB (DESY, Hamburg). The selected wavelength was  $\lambda = 0.138$  nm. The beam divergence in and out of the plane of reflection was set by two entrance cross-slits. The beam was focused to the size of (HxB)  $30 \times 60 \mu m^2$  (hence moderate micro-focus adapted to the gradient dimension) by using an assembly of refractive beryllium lenses [14]. The sample was placed horizontally on a goniometer. A beam stop was used to block the direct beam in front of the detector. In addition, a second, point-like moveable beam stop was also used to block the specular peak intensities on detector. The whole gradient dimension was 1.4 mm. It was measured in 20 steps (each step size is  $70 \mu m$ ) starting at the part with 700 nm thickness and ending at the part with 10 nm film thickness. The incident angle was  $\alpha_i=0.72^\circ$ , which is well above the critical angles of the diblock polymer and the nanoparticles. In this geometry the beam can penetrate the full film and thus the scattering data give access to the information from inside the film and not only from the polymer films surface. The scattered intensity was recorded with a two-dimensional (2D) detector (MARCCD;  $2048 \times 2048$  pixel) positioned at  $D_{SD}=1.97$  m behind the sample.

## 3 RESULT AND DISCUSSIONS

Figure 3 shows a composite image of the recorded 2d intensities using  $\mu$ GISAXS. The gradient was scanned from largest to smallest film thickness ordered from left to right and from top to bottom in figure 3. To focus on the modulation of the intensity along the vertical direction (at

$q_y = 0$ ), starting near the Yoneda region, in figure 3 a zoom-in this part of the 2d intensity was selected. The intensity modulation along the vertical direction results from the desired long-ranged correlation. This modulation propagates towards the specular peak position (not shown in figure 3) i.e., to the higher  $q_z$  and loses intensity. One can see in figure 3 that the modulation decreases in amplitude from one row to another row and from left to right in each row of images.

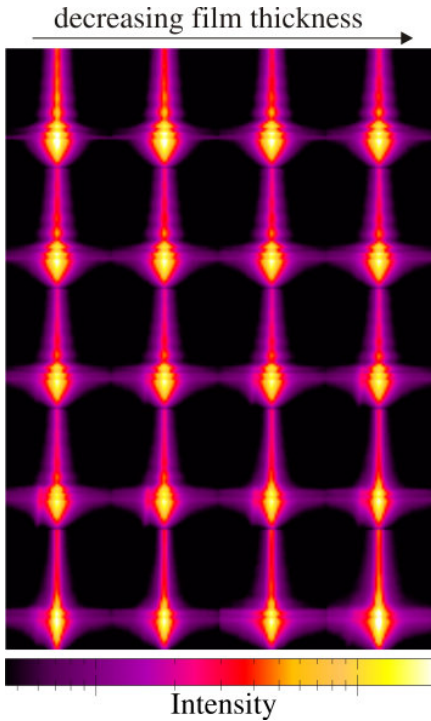


**Figure 3.** Composite image comprising the 2d scattering patterns from 20 positions along the thickness gradient (left to right and top to bottom). The top left scattering pattern was measured at the largest film thickness and the bottom right one at the smallest film thickness.

For better understanding of these scattering patterns vertical slice from the 2d intensity at  $q_y = 0$  are selected. These vertical cuts, frequently called detector scans, are plotted in figure 4. At the specular position the intensity drops due to shielding by the second beam stop. The cuts show that there is a well defined modulation in the intensity between the Yoneda and the specular peak (shielded) representing a roughness replication. This interface correlation is present in almost all areas of measurement (see all 2d images and all vertical cuts) i.e., from the thick to the thin area of the film. Consequently, the roughness of the substrate is reproduced by the composite film surface. Thus although nanoparticles are embedded in the diblock copolymer films, this long-ranged interface correlation is present. Both interfaces, the substrate and composite surface, are correlated starting from large lateral lengths down to a critical cut-off length even in presence of nanoparticles.

In a detector scan the intensity depends on the roughness of the sample and the chosen incident angle  $\alpha_i$ . In addition to the Yoneda and specular peak a modulation of the intensity in a detector scan is observed [15]. The spacing of the fringes in such modulation gives an estimation of the distance between the correlated interfaces  $d^{corr}$  [4] by the following a one dimensional Bragg condition [16] via

$$\Delta q_z = \frac{2\pi}{d^{corr}} \quad (1)$$

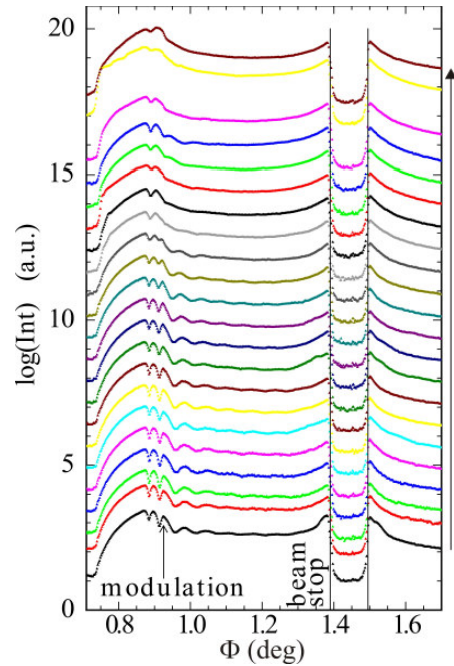


**Figure 4.** Vertical cuts of the 2d intensity at  $q_y = 0$ , called detector scans, plotted as a function of the detector angle  $\Phi = \alpha_i + \alpha_f$  with the exit angle, showing roughness correlation over a wide range of film thickness. The curves are shifted along y-axis neglecting their change in intensity values for clear presentation. From the bottom to the top the composite film thickness decreases.

With decreasing film thickness the amplitude of the modulation in the intensity decreases (see figure 4). Thus the roughness correlation decreases. The roughness correlation of thin films was determined by Andelmann et al [17] in the framework of a linear response theory. Following this approach, long wavelength fluctuations of the solid surface are followed by the liquid interface and short wavelength fluctuations are damped by the surface tension. With increasing film thickness the liquid interface becomes smoother and undulations of the solid surface are followed more closely as the film thickness decreases. Therefore the long-ranged correlation is expected to increase with decreasing film thickness, in contrary to the behavior observed in case of the nanocomposite films. However, the theory by Andelmann et al. focuses on simple liquids and thermodynamic equilibrium. In the present

investigation, instead of a simple liquid a composite polymer film with embedded nanoparticles is probed. Moreover, to achieve a maximum of long-ranged correlation no further processing was added to the spin coating and as a consequence the films are not in thermodynamic equilibrium.

In case of homopolymer and polymer blend films [4-12] the absence of thermodynamic equilibrium was addressed and it was shown, that the long-ranged correlations are due to frozen-in structures created during the spin-coating.

The in-plane cut-off length scale  $R_c$  is determined from the decay of the intensity modulations as a function of  $q_y$ . Thus vertical cuts parallel to detector cut are selected from the 2d intensity at different  $q_y$  components (see figure 5). As visible in figure 5 the amplitude of the modulations decreases with increasing  $q_y$  (from bottom to top in figure 5). The critical cut-off length is calculated by equation (2) as follows:

$$R_c = \frac{2\pi}{\Delta q_{corr}} \quad (2)$$

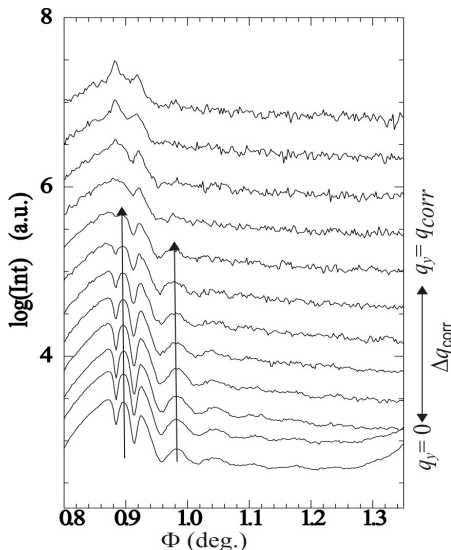


**Figure 5.** Example of vertical cuts from the 2d intensity cut at different  $q_y$  positions at one point along the gradient. For a better presentation the curves are shifted along vertical axis without maintaining the scale. At larger  $q_y$  the modulation decreases. No modulation is seen at  $q_{corr}$ .  $\Delta q_{corr}$  gives us directly the in-plane cut-off length scale  $R_c$ . The propagation of modulation is shown by two arrows.

At each position of the gradient the in-plane cut-off length scale  $R_c$  is determined.

## 4 CONCLUSION

A gradient nanocomposite thin film based on diblock copolymer P(S-b-I) matrix with embedded maghemite nanoparticles, which exhibits roughness correlation, has been successfully prepared by spin coating on top of solid support. Over the entire range of film thicknesses, from 10

to 700 nm, the long-ranged correlation between the substrate and the composite film surface is present. With decreasing film thicknesses this correlation decreases but is not vanishing. Thus in all cases a locally constant film thickness was established instead of only a mean constant film thickness. With respect to the application of thin nanocomposite films this is a key to the possibility of a reduced amount of necessary material.

## ACKNOWLEDGEMENT

We thank the Bavarian State Ministry of Sciences, Research and Arts for funding this research work through the International Graduate School “Materials Science of Complex Interfaces” (CompInt).

## REFERENCES

- [1] M. Bockstaller, R. Kolb and E. Thomas, *Adv. Mater.* 13, 1783, 2001.
- [2] W. Shenton, D. Pum, U. B. Sleytr, S. Mann, *Nature*, 389, 585, 1997.
- [3] P. Akora, R. M. Briber and P. Kofinas, *Polymer* 47, 2018, 2006.
- [4] P. Müller-Buschbaum and M. Stamm, *Macromolecules*, 31, 3686, 1998.
- [5] P. Müller-Buschbaum, J. S. Gutmann, C. Lorenz, T. Schmitt and M. Stamm, *Macromolecules*, 31, 9265, 1998.
- [6] M. Tolan, G. Vacca, J. Wang, S. K. Sinha, Z. Li, M. Rafailovich, J. Sokolov, A. Gibaud, H. Lorenz and J. P. Kotthaus, *Physica B*, 221, 53, 1996.
- [7] D. J. Stearns, *J. Appl. Phys.* 9, 4286, 1992.
- [8] E. E. Fullerton, J. Pearson, J. H. Sowers, S. D. Bader, X. Z. Wu and S. K. Sinha, *Phys. Rev. B* 48, 17432, 1993.
- [9] A. Gibaud, N. Cowlam, G. Vignaud and T. Richardson, *Phys. Rev. Lett.* 74, 3205 1995.
- [10] V. Nitz, M. Tolan, J. P. Schlomka, O. H. Seeck, J. Stettner, W. Press, M. Stelzle and E. Sackmann, *Phys. Rev. B*, 54, 5038, 1996.
- [11] E. A. Mol, J. D. Shindler, A. N. Shalaginov and H. W. de Jeu, *Phys. Rev. B*, 54, 536, 1996.
- [12] E. A. Mol, G. C. L. Wong, J. M. Petit, F. Rieutord and H. W. de Jeu, *Phys. Rev. Lett.* 79, 3439, 1997.
- [13] P. Müller-Buschbaum, *Anal. Bioanal. Chem.* 376, 3, 2003.
- [14] S. V. Roth et al., *Review Of Scientific Instruments* 77, 085106, 2006.
- [15] J. Stettner, L. Schwalowsky, O. H. Seeck, M. Tolan, W. Press, C. Schwarz and H. v. Känel, *Phys. Rev. B* 53, 1398, 1996.
- [16] V. Holý and T. Baumbach, *Phys. Rev. B* 49, 10668, 1994.
- [17] D. Andelmann, J. F. Joanny and M. O. Robbins, *Europhys. Lett.* 7, 731, 1988.